

Research Article

Investigation of Tribological Behaviour on DLC Coatings for AA5051 using DC Sputtering

L. Natrayan ¹, Piyush Gaur,² Anjibabu Merneedi ³, S. Kaliappan ⁴, Pravin P. Patil,⁵
V. Sivaprakash ⁶, and Muse Degefe Chewaka ⁷

¹Department of Mechanical Engineering, Saveetha School of Engineering, SIMATS, Chennai 602105, India

²School of Engineering, Bidholi Campus, University of Petroleum and Energy Studies, Dehradun, Uttarakhand 248002, India

³Department of Mechanical Engineering, Aditya College of Engineering, Surampalem, Andhra Pradesh, India

⁴Department of Mechanical Engineering, Velammal Institute of Technology, Chennai, Tamil Nadu, India

⁵Department of Mechanical Engineering, Graphic Era Deemed to be University, Bell Road, Clement Town, 248002 Dehradun, Uttarakhand, India

⁶Department of Mechanical Engineering, Sathyabama Institute of Science and Technology, Chennai, Tamil Nadu, India

⁷Department of Mechanical Engineering, Ambo Institute of Technology-19, Ambo University, Ethiopia

Correspondence should be addressed to L. Natrayan; nat07.sl@icloud.com
and Muse Degefe Chewaka; muse.degefe@ambou.edu.et

Received 25 February 2022; Accepted 16 May 2022; Published 27 May 2022

Academic Editor: S.K. Khadheer Pasha

Copyright © 2022 L. Natrayan et al. This is an open access article distributed under the Creative Commons Attribution License, which permits unrestricted use, distribution, and reproduction in any medium, provided the original work is properly cited.

DLC coatings are deposited on aluminium substrates to improve the wear resistance property of the substrates using sputtering deposition in this study. DLC coatings are deposited using the graphite target onto the Al5051 substrates using DC sputtering. The deposited coatings are then analyzed for their adhesion strength, hardness, coefficient of friction, and chemical compositions. The pin-on-disk method is conducted in vacuumed conditions, dry air conditions (0% RH), and ambient air conditions (40% RH). The different testing conditions have shown different results for the same testing sample. This indicates the nature of DLC film adsorption in ambient air conditions. The chemical composition study has further revealed the adsorbing compounds and the ability of hydrogen and water molecules to get adsorbed on the thin-film surface. This study gives insight into the effect of molecules present in the ambient air on the performance of DLC coatings. It investigates the effect of three DLC coatings deposited using the graphite target onto the Al5051 substrates using DC sputtering.

1. Introduction

Surface engineering is a critical study for any machine/part. Retaining surface properties without wearing down quickly is essential for a longer life of the machine [1]. For machines made of softer materials like aluminium and other materials, the surface is softer without offering any resistance to wear off over time [2]. There are many methods to improve the hardness and strength of the material like stress hardening and shot-peening. Still, these methods are inefficient in effectively improving the wear resistance and improving the lubrication simultaneously [3]. The coatings are proposed on the substrates. When deposited on the substrate surface,

these coatings are hard and act as lubricants. Diamond-like carbon (DLC) is a coating made up of carbon particles having strength equivalent to that of diamond [4]. These coatings have strong SP_3 bonds, resulting in higher strength than the graphite and other amorphous carbon coatings. Thus, CVD methods were widely employed to grow DLC films because they got ultrasoft and defect-free coatings over large areas and irregular shapes [5]. Due to these bonds, DLC coatings have exceptional tribological properties like great corrosion resistance, higher hardness, low friction coefficient, and elevated wear resistance in harsher conditions [6]. Solid graphite is used as the target material for the growth of DLC through PVD methods, whereas high

pure hydrocarbon gases are used in the case of CVD methods. Thus, the DLC films grown under PVD methods are hydrogen free. On the other hand, hydrogen is an inherently inevitable component in CVD-grown DLC films. Due to these properties, DLC is being widely used in many industrial applications. The tribological qualities of DLC films have aroused interest in the research community for quite a long time [7]. Lower deposition temperatures and easier substrate adherence are benefits of DLC films. DLC coating's antisticking properties, as well, have piqued interest in their usage on aluminium alloys. It is widely used as a wear-resistant protective coating in magnetic storage, vehicle, tooling, biomedical, and other industries due to its unique features [8]. DLC electrochemical resistance has also been seen as a desirable property. Film composition and structure, which rely on the deposition process and precursor gas, influence DLC electrochemical corrosion behaviour [9]. Many experiments have been conducted to improve the quality of DLC coatings by including additional foreign components into the structure. These films have high internal stresses, resulting in poor adhesion. The use of silicon as a coating dopant and an amorphous silicon interlayer aids in the resolution of this issue, enhancing the system's load-bearing capacity [10]. Amorphous carbon compounds with diamond-like characteristics are known as diamond-like carbon coatings. DLC coatings can be amorphous, more or less flexible, hard, strong, and slippery, depending on the composition and manufacturing process. Films can be made by plasma-assisted chemical vapour deposition, ion beam deposition, sputter deposition, and RF plasma deposition [11]. Although the strength of DLC coating comes from the strong SP_3 bonds, DLC coating comprises both SP_2 and SP_3 bonds. Besides these bonds, DLC coating comprises small amounts of hydrogen [12]. This hydrogen is chemically adsorbed into the DLC coating. There have been numerous studies undertaken to identify what causes the differences in tribological behaviour of different types of DLC films [13]. The bond structure influences the tribological behaviour of these coatings. Whether with or without hydrogen, hydrogen and water and other test atmospheres play a crucial role in changing the tribological behaviour of DLC coatings [14]. The hydrogen concentration, the SP_2/SP_3 ratio, and the presence or absence of doping elements in DLC films all affect the tribological features of the films [15].

DLC film's friction and wear qualities are highly influenced by their structures and compositions. Hydrogenated amorphous carbon films, in particular, are of particular interest since some of them have a friction coefficient of less than 0.01, which can drop to 0.001 in high-vacuum or inert settings due to the production of tribofilms on the counter sides [16]. Not all films result in extremely low friction. In high vacuum settings, films were reported to have a very low or extremely high friction coefficient. A film with low hydrogen content could not have an exceptionally low friction coefficient, compared with a film with a high hydrogen concentration [17]. As a result, the hydrogen content of DLC films is thought to play an important role in super low friction. Furthermore, DLC films' super low friction is dependent on the sliding environment [18]. The films were less than 0.01 under ultrahigh vacuum (10^{-6} Pa), but the

friction coefficient dramatically rose after 100-200 cycles. In hydrogen, on the other hand, super low friction is maintained for 1000 cycles at gas pressures ranging from 50 to 1000 Pa [19]. This study proved that the physical properties of the counter body are more important than the chemical reactions and testing environment. Studies on hydrogenated DLC films against Si_3N_4 and Al_2O_3 in a vacuum later than the former showed lower friction.

This study gives insight into the effect of molecules present in the ambient air on the performance of DLC coatings. It investigates the effect of three DLC coatings deposited using the graphite target onto the Al5051 substrates using DC sputtering. The deposited coatings are then analyzed for their adhesion strength, hardness, coefficient of friction, and chemical compositions. The pin-on-disk method is conducted in vacuumed conditions, dry air conditions (0% RH), and ambient air conditions (40% RH). The mass spectroscopy analysis of evolved gases during tribology studies of DLC films showed the signature of CO_2 formation in dry air and hydrocarbon or carboxyl groups while testing under a humid environment. These studies emphasize the significance of understanding the tribochemical interactions that occurred during tribotesting of DLC films.

2. Methodology

Graphite targets were deposited on aluminium using the DC-sputtering method. For the full set of experiments, graphite targets with a purity of 99.99%, a diameter of 30 mm, and a thickness of 5.0 mm were obtained and used. Figure 1 shows the experimental system's schematic design [20]. The RF power supply is connected to the magnetron on which the target material to be coated is put. The entire chamber is grounded, and the magnetron acts as an electrode. The sputtering voltage was set to 400 V in this experiment, while the current was kept below 1 A [21].

Aluminium is cut into $10 \times 10 \times 1$ mm coupons which are developed and utilized for further experiments. These samples are made experiment ready by removing impurities by acetone cleaning. And they are further atomically cleaned by plasma etching for 15 minutes before sputtering. Two-stage pumps maintain the vacuum at 10^{-2} mbar inside the chamber. The substrate's temperature is kept constant at room temperature. The substrate temperature is monitored and can be adjusted manually by the substrate holder [22]. A total thickness of 1000 nm is attained for the DLC thin films. The mechanical characteristics of the film are investigated using a nanoindentation method (hardness and modulus). Samples are heated for resin stabilization. The Agilent Technologies machine is utilized for Berkovich indenter indentations in nanoindentation processes [23]. The samples are scratch tested to determine the adherence of the produced DLC coatings. The scratch analysis with the Berkovich indenter is done on the same system used for nanoindentation. The load gradually increases to determine the critical load at which the DLC coating begins to peel off. This force is the ultimate load and determines the film's adhesion strength. The chemical composition of the coating is determined via XRD analysis on DLC samples [24].

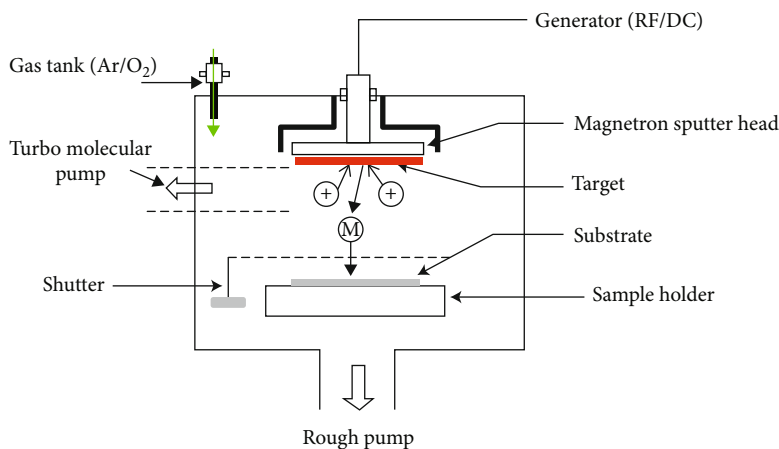


FIGURE 1: Sputtering rig.

TABLE 1: Hardness values of DLC coatings.

Sample	1	2	3	4	5	6	7	8
Load ($\frac{1}{4}$ N)	10422	10424	10423	10422	10422	10424	10422	10425
Hardness (GPa)	5.2	4.9	5.1	5.1	5.2	5.0	5.1	5.1
Modulus (GPa)	89	88	90	90	90	89	88	89

The pin-on-disk method is used to determine the wear and friction of the samples. The pin is an uncoated aluminium sample, while the disk is an aluminium sample coated with DLC. The test is carried out with a load of 100 gm and a total revolution count of 500. The DLC-coating behaviour is adsorbed with hydrogen and water vapour conditions; the pin-on-disk method is conducted in a vacuumed condition, dry air condition (0% RH), and ambient air condition (40% RH). The testing included ambient and dry air (40% RH and 0% RH, respectively), nitrogen, and a hydrogen-helium mixture (40 vol % H_2 -60 vol % He). Before adding the nitrogen, the chamber was evacuated to a pressure of 3.99×10^3 Pa or below [25].

Before the gas was pumped into the working chamber, the chamber was maintained at a vacuum pressure of 3.99×10^3 Pa and pumped with nitrogen, and then, the vacuum was brought to the same pressure level again to remove any remaining air and water vapours. All tests were carried out at a pressure of 1 atm [26].

3. Results and Discussion

3.1. Hardness. Eight samples have been developed by DLC coating in two sets. All samples have been deposited with DLC coating with the same parameters in a single rig. These coatings are then tested for their mechanical properties hardness and elastic modulus with a nanoindentation setup using a Berkovich indenter. The hardness and elastic modulus of the samples calculated are given in Table 1. Because of the rigidity of the DLC coating, the load can be transferred directly to the substrate [27]. The substrates deform elastically when a load is applied, and the hardness under the load is measured. According to the findings in this case, the com-

bined hardness of the coating and substrate causes a significant loss in the coating's future qualities. A battery of tests was performed on each sample to determine its average hardness and modulus of elasticity. The indentation area after the load has been removed from the surface, and the maximal stresses applied for that specific experiment are considered for estimating hardness. At maximum load, all of the experiments were held for 10.0 seconds [28].

The hardness of the samples varied from 5.0 to 5.2 GPa, and the modulus of the DLC coatings varied from 88 GPa to 90 GPa. The minute difference in the hardness and modulus is attributed to the vacuum chamber's sample placement position. As the sample position changes inside the chamber, the glancing angle of the depositing atoms changes. The glancing angle of the depositing atoms has a slight effect on the thin film's hardness [29]. The atoms depositing perpendicular to the substrate surface hits the surface with the highest kinetic energy, and the impact leads to loss of energy. At the same time, the atoms depositing with an angle less or greater than the perpendicular angle have less impact energy loss and arrange themselves on the depositing surface [30]. The presence of defects in the thin film can be determined by using nanoindentation data. The data set points obtained during the nanoindentation process are plotted in a load vs. deflection graph. The load vs. deflection graph of one of the samples is given in Figure 2. A high C/H ratio results in a high growth rate and less hydrogen content. On the other hand, a lower C/H ratio reduces the growth rate and increases the hydrogen content. Moreover, the presence or absence of hydrogen further influences the bonding state and the mechanical properties of the DLC film. However, CH_4 was preferred over the other two due to its availability and pure high state, which reduces contamination necessary

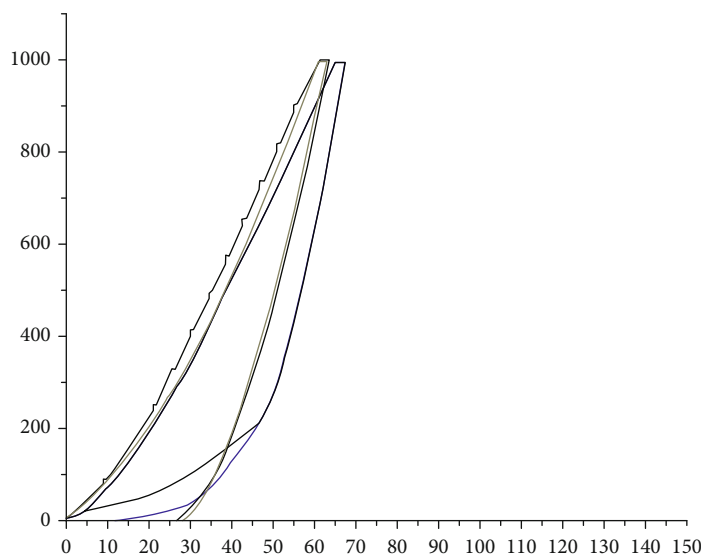


FIGURE 2: Load vs. deflection curve of DLC thin film measured using nanoindentation.

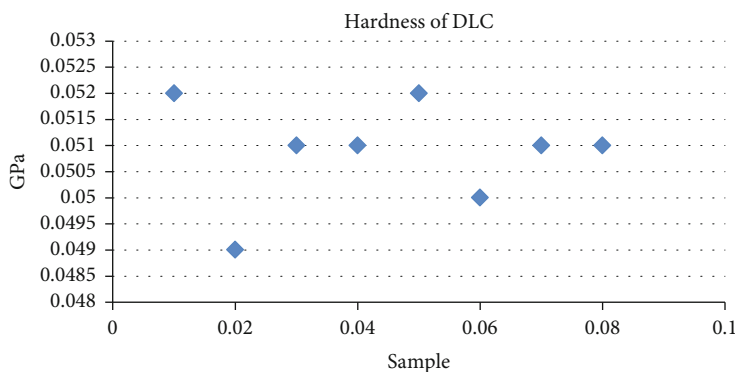


FIGURE 3: Hardness of DLC.

for electronics applications. Moreover, it also helps stabilize the SP_3 bonding due to the high fraction of hydrogen. This is required for improving mechanical properties [31].

A specimen hardness test is usually performed to extract hardness and modulus data. There are two types of traditional hardness tests: Rockwell and Brinell tests. A known particular load is applied to the surface in both tests, and an indentation is formed with an indenter. The indentation formed on the sample is used to determine the hardness. However, because the film thickness is so thin in thin-film applications, the values obtained will be influenced by the thin film and the substrate [32]. Thin films must be indented up to 10% of their thickness, after which the substrate qualities modify the values. As the thickness of the DLC films developed in the current study is around $1000n$, care is taken that the indentation's depth does not cross the 10% thickness [33]. The integrity of each indentation of the load-displacement data was evaluated. Load displacement plots with a "jump" or numerous "jumps" in the indentation depth are observed in Figure 2.

The hardness of DLC is shown in Figure 3. The origin of these leaps is unknown; however, subsurface defects during force-driven indentation testing are most likely to blame.

This defect would account for the observed behaviour: a sudden increase in depth with no change in measured load [34]. As a result, the measured contact depth and corresponding contact area were wrongly calculated. Their larger maximum indentation depth can identify the majority of those irregular curves. Removing discontinuous indentation curves from the data set and those that violate the scale's repeatability criteria is crucial. The indenter penetrating the surface layers is as little as 60 nm at the 1000 N peak load, leaving a residual impression of less than $15n$ after load removal, demonstrating the hardness of the coating generated [35]. This hardness can be due to the formation of SP_3 bonds or the interlinking of SP_2 bonds between carbon atoms.

The hardness values of the samples measured are plotted on a graph above. The points scattered are concentrated on the value 5.1 GPa, and this value can be taken as the mean value and can be further selected as the hardness of developed DLC coatings.

3.2. Chemical Composition. The DLC coating contains amorphous carbon, according to the XRD analysis. The sample is stored in an XRD machine and swept from 200 to 900 degrees for analysis. Other than carbon, there are

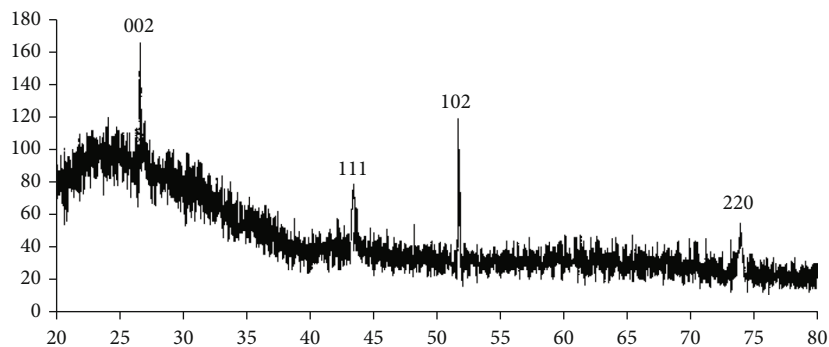


FIGURE 4: XRD graph of DLC coating on Al.

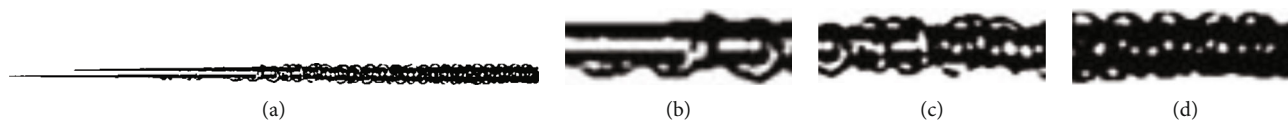


FIGURE 5: Scratch developed on DLC film.

no other peaks. The carbon films' X-ray diffraction pattern is shown in Figure 4. The larger peak in Figure 4 denotes that these films are nanocrystalline. There are four diffraction peaks in the spectra at 2θ values, as shown in the diagram. The peaks at 2θ values of 26.66° and 51.9° correspond to the reflection from (002) and (102) planes of graphite, respectively, and the peaks at 2θ values of 43.52° and 73.94° correspond to the (111) and (220) lattice spacing of cubic diamond, respectively [36]. Tuning the surface chemistry and passivating unsaturated dangling bonds to avoid adhesive covalent interaction between mating parts and further reducing friction and wear are of scientific importance. Recent studies on the molecular level interaction of DLC films showed that surface reactivity mostly controls friction behaviour and hydrogen-terminated DLC films possessed an ultralow friction coefficient [37].

3.3. Adhesion Test. The damage evolution on the DLC film while scratching under a progressive applied normal load is shown in Figure 5. During nanoscratch testing on the DLC-coated system, the measured coefficient of friction increases linearly with a normal load. The surface image reveals that the width of the scratch track and the level of surface damage increase with normal load, explaining the observed friction effect. After the test shows the general scratch on the DLC coating, the first damage mark may be seen at the margin of the scratch line in Figure 5(b). The emergence of the first flaking is depicted in Figure 5(c), and the appearance of the total failure of the DLC on the surface is depicted in Figure 5(d).

The different loads where the coatings have peeled off have been given in Table 2.

The minute difference in the recorded ultimate loads can be attributed to the nanodefects present in the coatings and the position of the samples placed inside the vacuum chamber during the deposition process. The glancing angle of the depositing atoms changes as the sample position inside the chamber changes. The hardness of the thin coating is

TABLE 2: Ultimate loads where coatings peeled off the substrate during the scratch test.

Sample	1	2	3	4	5	6	7	8
Load ($\frac{1}{4}$ N)	35.2	35.3	35.2	35.1	35.2	35.2	35.1	35.2



FIGURE 6: Wear track on DLC coating deposited on Al substrate.

affected by the glancing angle of the depositing atoms. The atoms depositing perpendicular to the substrate surface collide with the surface with the highest kinetic energy, resulting in energy loss. Atoms depositing at an angle less than or equal to the perpendicular lose less energy and organize themselves on the depositing surface. Recent findings showed that stainless steel balls used against the DLC film get oxidized in a humid environment, and no signs of oxidation were seen in dry air or oxygen medium. It is due to the formation of electrochemical galvanic corrosion cells by the tribochemical interactions.

3.4. Pin-on-Disk Test. The pin-on-disk tribometer was used to investigate the DLC coatings' friction qualities. Figure 6

TABLE 3: Wear test results of coatings.

Sample	Friction coefficient	Width of track (μm)	Loss of volume (m^3)	Wear coefficient (K)
Aluminium substrate	0.95	1.5	4.85×10^{-9}	7.52×10^{-5}
1	0.03	230	1.8×10^{-11}	3.02×10^{-6}
2	0.03	230	1.8×10^{-11}	3.02×10^{-6}
3	0.04	235	1.8×10^{-11}	3.02×10^{-6}
4	0.04	238	1.8×10^{-11}	3.02×10^{-6}
5	0.03	230	1.8×10^{-11}	3.02×10^{-6}
6	0.03	230	1.8×10^{-11}	3.02×10^{-6}
7	0.04	236	1.8×10^{-11}	3.02×10^{-6}
8	0.03	230	1.8×10^{-11}	3.02×10^{-6}

TABLE 4: Wear behaviour of DLC in various conditions.

RH	Friction coefficient	Width of track (μm)	Loss of volume (m^3)	Wear coefficient (K)
0	0.03	230	1.8×10^{-11}	3.02×10^{-6}
40%	0.01	190	0.98×10^{-11}	1.86×10^{-6}

depicts the experimental outcomes. For the aluminium base substrate used as a reference, the stable coefficient of friction (COF) was around 0.95. The samples coated with DLC layers exhibited a significant reduction in COF, with values ranging from 0.04 to 0.03. The friction coefficient values are lower than those found in the literature, where the friction coefficient of the DLC coating increased continuously and eventually achieved a value of 0.2.

In contrast, the DLC sample's friction coefficient reached 0.3 at the end of the test. On the other hand, the friction coefficients are remarkably similar to those described in the literature. According to this study, the resultant coefficients of friction are closely connected to the carbon concentration and crystal phases. A significant point to note is that all coatings had nearly consistent friction coefficients at the end of the test, indicating that none of them was worn down. The microwave generated at the source reaches the processing chamber via circulator, traverses inside a rectangular waveguide, and finally passes through the dielectric window. The circulator is connected mainly to protect the microwave source from the reflected waves. Once the microwave enters the rectangular waveguide, it converts into a rectangular mode. The rectangular waveguide consists of 3 stub tuners to tune the microwave's waveform. A water-cooled antenna located at the end of the waveguide converts the microwave into a circular mode and pushes it into the process chamber through a quartz window. The process chamber is the resonance zone where the energy transfer occurs between the microwave and stray electrons. A tunable electromagnet sits over the process chamber to get an 875-gauss magnetic field required for creating resonance. The energized electrons further contribute toward plasma generation. The plasma further extends to the deposition chamber due to the spread of the divergent magnetic field and helps the film's growth.

Furthermore, the wear tracks on the DLC coatings were substantially narrower than those on the reference substrate. According to this, the track width of the uncoated aluminium substrate was roughly 1.5 mm on average, whereas the DLC track width was 230 m. Optical micrographs of the ensuing wear tracks for both DLC-coated samples are shown in Figure 6. The wear tracks of the sample coated with DLC revealed a surface with less abrasive wear, which is worth noting. The coated samples' resultant groove dimensions were several orders of magnitude less than the uncoated reference sample (aluminium). The wear coefficient is calculated according to ASTM G99-95 and is a function of the loss volume along the entire track using the track width, normalized by the applied force and total sliding distance. Table 3 summarizes the findings. Table 3 summarizes the different results for each analyzed sample in terms of friction coefficient, wear track width, loss volume, and wear coefficient. The untreated sample had a wear coefficient of $7.52 \times 10^{-5} \text{ mm}^3/\text{nm}$, whereas DLC coatings had a wear coefficient of $3.02 \times 10^{-6} \text{ mm}^3/\text{nm}$, almost two orders of magnitude lower than the reference substrate.

3.5. Effect of Hydrogen Adsorption on Properties of DLC.

Table 4 gives the comparison results of the DLC thin film tested in different humidity conditions. Vacuum and 40% RH (relative humidity) conditions are used to run the pin-on-disk test for the DLC thin film on an Al substrate. The 40% RH values are identical to the one we obtained in atmospheric condition as both have the same humidity values.

It is evident from Table 4 that the environmental humidity and the other environmental conditions play a crucial role in the friction properties of the DLC films. The humidity present in the atmosphere or, in the present case, in the testing atmosphere is adsorbed by the DLC film, and the

friction is reduced. Literature has looked into the microstructure of the graphitized layer, and it has been discovered that graphite particles expand slowly after nucleation, implying that they form in isolated hot spots. When a thin graphitized tribolayer is formed, friction was reduced, but the DLC film remained intact. These oscillations in the DLC layer during friction throughout the steady-state phase of the studies confirm graphitization and reduced friction. The low friction coefficient attained in the 40% RH test is due to the formation of a graphitized tribolayer between the pin-and-disk materials and low shear strength between hexagonal planes in the graphite structure. Under these conditions, the wear process can be conceived of as a low-rate continuous consumption with the production of graphitized tribofilm. Plasma treatment of DLC films is an effective method to alter the surface chemistry in a controlled manner to get a terminated surface with desired surface reactivity required to tune the wettability characteristics. In recent times, DLC has emerged as the most renowned wear-resistant coating material and has become a part of several appliances. However, modernization demands multifunctional devices in a miniaturized form where DLC films with versatile properties come in handy. Therefore, it brings an opportunity to have a relook into this amazing material for tailoring the properties suitable for these applications. Although great scientific reports on various aspects of the DLC films are readily available, certain scientific aspects are yet to be addressed. A few studies have focused on a detailed analysis of the wear tracks to establish the mechanism responsible for the ultralow friction coefficient. Not many studies are found in tuning surface chemistry by functionalization or passivation towards achieving superior tribological properties. Tuning the surface energy of DLC films is an important concern in tribology and biomedical implants. Plasma exposure conditions need to be optimized to achieve superior properties for the above applications.

The first test was conducted in a dry environment (0% RH). The experimental results revealed extremely low friction values and a high rate of wear on the pin and DLC film, all of which were compatible with increased graphitization during friction. The low friction coefficient in a substantial portion of the friction process can be attributable to the low wear rates of pin and DLC-coated disks. The results of experiments 0% RH and 40% RH show that the humidity of the atmosphere has a considerable impact on the graphitization process of the DLC film. By modifying the composition at the pin/disk contact interface, humidity might affect the friction process. The involvement of hydrogen atoms in contact bonding between the DLC film and its counterface is evident.

4. Conclusion

This study has successfully deposited DLC coatings on an Al substrate using DC sputtering. The deposited coatings are evaluated for their hardness, adhesion, and friction properties. The developed films have nanodefected developed during the deposition process and are identified during nanoindentation analysis. The humidity factor influences the friction

property of the films in the testing environment. The DLC film absorbs the humidity present in the atmosphere. The humidity adsorbed reduces the friction resistance of the film and improves the sliding nature.

Data Availability

The data used to support the findings of this study are included in the article. Should further data or information be required, these are available from the corresponding author upon request.

Conflicts of Interest

The authors declare that there are no conflicts of interest regarding the publication of this paper.

Acknowledgments

The authors thank Saveetha School of Engineering, SIMATS, Chennai for the technical assistance. The authors appreciate the support from Ambo University, Ethiopia.

References

- [1] B. Aramide, S. Pityana, R. Sadiku, T. Jamiru, and P. Popoola, "Improving the durability of tillage tools through surface modification—a review," *The International Journal of Advanced Manufacturing Technology*, vol. 116, no. 1-2, pp. 83–98, 2021.
- [2] M. N. Brykov, I. Petryshynets, M. Džupon et al., "Microstructure and properties of heat affected zone in high-carbon steel after welding with fast cooling in water," *Materials*, vol. 13, no. 22, p. 5059, 2020.
- [3] T. Gittler, M. Glasder, E. Öztürk, M. Lüthi, L. Weiss, and K. Wegener, "International conference on advanced and competitive manufacturing technologies milling tool wear prediction using unsupervised machine learning," *The International Journal of Advanced Manufacturing Technology*, vol. 117, no. 7-8, pp. 2213–2226, 2021.
- [4] H. Shagwira, T. O. Mbuya, F. M. Mwema, M. Herzog, and E. T. Akinlabi, "Taguchi optimization of surface roughness and material removal rate in CNC milling of polypropylene+5wt.% quarry dust composites," *IOP Conference Series: Materials Science and Engineering*, vol. 1107, no. 1, p. 012040, 2021.
- [5] M. Čavić, M. Penčić, D. Oros, D. Čavić, M. Orošnjak, and M. Rackov, "High-capacity stacking apparatus for thermoforming machine—part I: synthesis of intermittent mechanisms as stacker driving units," *Advances in Mechanical Engineering*, vol. 13, no. 8, 2021.
- [6] S. Vellaiyan, A. Subbiah, S. Kuppasamy, S. Subramanian, and Y. Devarajan, "Water in waste-derived oil emulsion fuel with cetane improver: formulation, characterization and its optimization for efficient and cleaner production," *Fuel Processing Technology*, vol. 228, article 107141, 2022.
- [7] B. H. Bejaxhin, G. Paulraj, and M. Prabhakar, "Inspection of casting defects and grain boundary strengthening on stressed Al6061 specimen by NDT method and SEM micrographs," *Journal of Materials Research and Technology*, vol. 8, no. 3, pp. 2674–2684, 2019.

- [8] V. S. Ponnappan, B. Nagappan, and Y. Devarajan, "Investigation on the effect of ultrasound irradiation on biodiesel properties and transesterification parameters," *Environmental Science and Pollution Research*, vol. 28, no. 45, pp. 64769–64777, 2021.
- [9] P. Asha, L. Natrayan, B. T. Geetha et al., "IoT enabled environmental toxicology for air pollution monitoring using AI techniques," *Environmental Research*, no. article 112574, 2022.
- [10] Y. Devarajan, B. T. Nalla, M. Dinesh Babu, G. Subbiah, R. Mishra, and S. Vellaiyan, "Analysis on improving the conversion rate and waste reduction on bioconversion of *Citrullus lanatus* seed oil and its characterization," *Sustainable Chemistry and Pharmacy*, vol. 22, article 100497, 2021.
- [11] H. Z. Nabi and T. Aized, "Performance evaluation of a carousel configured multiple products flexible manufacturing system using Petri net," *Operations Management Research*, vol. 13, no. 1-2, pp. 109–129, 2020.
- [12] U. Koklu, S. Morkavuk, C. Featherston et al., "The effect of cryogenic machining of S2 glass fibre composite on the hole form and dimensional tolerances," *The International Journal of Advanced Manufacturing Technology*, vol. 115, no. 1-2, pp. 125–140, 2021.
- [13] R. D. S. Rawendra and V. O. Puspita, "Use of six sigma methods to reduce packaging defect in sweetened condensed milk sachets: a case study in XYZ milk industry, Indonesia," *IOP Conference Series: Earth and Environmental Science*, vol. 426, no. 1, p. 012174, 2020.
- [14] T. Zhang, S. Liu, X. Zhang et al., "Fabrication of two-dimensional functional covalent organic frameworks via the thiol-ene "click" reaction as lubricant additives for antiwear and friction reduction," *ACS Applied Materials & Interfaces*, vol. 13, no. 30, pp. 36213–36220, 2021.
- [15] C. Hu, D. Ashok, D. R. Nisbet, and V. Gautam, "Bioinspired surface modification of orthopedic implants for bone tissue engineering," *Biomaterials*, vol. 219, article 119366, 2019.
- [16] A. Erdemir and J. M. Martin, "Superior wear resistance of diamond and DLC coatings," *Current Opinion in Solid State and Materials Science*, vol. 22, no. 6, pp. 243–254, 2018.
- [17] H. Cicek, A. Keles, Y. Totik, and I. Efeoglu, "Adhesion and multipass scratch characterization of Ti:Ta-DLC composite coatings," *Diamond and Related Materials*, vol. 83, pp. 80–86, 2018.
- [18] J. A. García, P. J. Rivero, E. Barba et al., "A comparative study in the tribological behavior of DLC coatings deposited by HiPIMS technology with positive pulses," *Metals*, vol. 10, no. 2, p. 174, 2020.
- [19] K. C. Mutyala, Y. A. Wu, A. Erdemir, and A. V. Sumant, "Graphene - MoS₂ ensembles to reduce friction and wear in DLC-steel contacts," *Carbon*, vol. 146, pp. 524–527, 2019.
- [20] F. O. Kolawole, S. K. Kolawole, L. B. Varela, A. F. Owa, M. A. Ramirez, and A. P. Tschiptschin, "Diamond-like carbon (DLC) coatings for automobile applications," *Engineering Applications of Diamond*, 2020.
- [21] E. Marin, A. Lanzutti, M. Nakamura et al., "Corrosion and scratch resistance of DLC coatings applied on chromium molybdenum steel," *Surface and Coatings Technology*, vol. 378, article 124944, 2019.
- [22] X. Wei, L. Chen, M. Zhang, L. Zhibin, and G. Zhang, "Effect of dopants (F, Si) material on the structure and properties of hydrogenated DLC film by plane cathode PECVD," *Diamond and Related Materials*, vol. 110, article 108102, 2020.
- [23] F. Sanchette, M. El Garah, S. Achache et al., "DLC-based coatings obtained by low-frequency plasma-enhanced chemical vapor deposition (LFPECVD) in cyclohexane, principle and examples," *Coatings*, vol. 11, no. 10, p. 1225, 2021.
- [24] K. Sakurai, M. Hiratsuka, H. Nakamori, K. Namiki, and K. Hirakuri, "Evaluation of sliding properties and durability of DLC coating for medical devices," *Diamond and Related Materials*, vol. 96, pp. 97–103, 2019.
- [25] Y. Yu, Y. Sha, Y. Jianming et al., "DLC(sa) and DLCA(sa) pre-treatments boost the efficiency of microbial lipid production from rice straw via *Trichosporon dermatis*," *Fuel*, vol. 309, article 122117, 2022.
- [26] A. Modabberasl, M. Sharifi, F. Shahbazi, and P. Kameli, "Multi-fractal analysis of DLC thin films deposited by pulsed laser deposition," *Applied Surface Science*, vol. 479, pp. 639–645, 2019.
- [27] D. Tobała, T. Liskiewicz, L. Yang, T. Khan, and Ł. Boroń, "Effect of mechanical and thermochemical tool steel substrate pre-treatment on diamond-like carbon (DLC) coating durability," *Surface and Coatings Technology*, vol. 422, article 127483, 2021.
- [28] D. Wu, S. Ren, P. Jibin, L. Zhibin, G. Zhang, and L. Wang, "A comparative study of tribological characteristics of hydrogenated DLC film sliding against ceramic mating materials for helium applications," *Applied Surface Science*, vol. 441, pp. 884–894, 2018.
- [29] D. Damodharan, K. Gopal, A. P. Sathiyaganam, B. Rajesh Kumar, M. V. Depoures, and N. Mukilarasan, "Performance and emission study of a single cylinder diesel engine fuelled with n-octanol/WPO with some modifications," *International Journal of Ambient Energy*, vol. 42, no. 7, pp. 779–788, 2021.
- [30] M. Anjibabu, L. Natrayan, S. et al., "Experimental investigation on mechanical properties of carbon nanotube-reinforced epoxy composites for automobile application," *Journal of Nanomaterials*, vol. 2021, Article ID 4937059, 7 pages, 2021.
- [31] Y. Devarajan, D. B. Munuswamy, B. T. Nalla, G. Choubey, R. Mishra, and S. Vellaiyan, "Experimental analysis of *Sterculia foetida* biodiesel and butanol blends as a renewable and eco-friendly fuel," *Industrial Crops and Products*, vol. 178, article 114612, 2022.
- [32] L. Natrayan, A. Merneedi, G. Bharathiraja, S. Kaliappan, D. Veeman, and P. Murugan, "Processing and characterization of carbon nanofibre composites for automotive applications," *Journal of Nanomaterials*, vol. 2021, Article ID 7323885, 7 pages, 2021.
- [33] A. B. H. Bejaxhin, G. Paulraj, and S. Aravind, "Influence of TiN/AlCrN electrode coatings on surface integrity, removal rates and machining time of EDM with optimized outcomes," *Materials Today: Proceedings*, vol. 21, pp. 340–345, 2020.
- [34] M. Karthick and K. Yoganandam, "Investigation of mechanical properties and corrosion performance of CNT coated on EN8 mild steel," *Materials Today: Proceedings*, vol. 46, pp. 4224–4227, 2021.
- [35] A. B. H. Bejaxhin and G. Paulraj, "Experimental investigation of vibration intensities of CNC machining centre by microphone signals with the effect of TiN/epoxy coated tool holder," *Journal of Mechanical Science and Technology*, vol. 33, no. 3, pp. 1321–1331, 2019.

- [36] L. Natrayan, A. Merneedi, D. Veeman et al., "Evaluating the mechanical and tribological properties of DLC nanocoated aluminium 5051 using RF sputtering," *Journal of Nanomaterials*, vol. 2021, Article ID 8428822, 7 pages, 2021.
- [37] V. Sivaprakash, L. Natrayan, R. Suryanarayanan, R. Narayanan, and P. Paramasivam, "Electrochemical anodic synthesis and analysis of TiO₂ nanotubes for biomedical applications," *Journal of Nanomaterials*, vol. 2021, Article ID 9236530, 10 pages, 2021.